

One-Dimensional Molecular Zippers

Hyo Won Kim,^{†,‡,#} Jaehoon Jung,^{‡,§} Mina Han,^{||} Seongjoon Lim,[†] Kaoru Tamada,[⊥] Masahiko Hara,^{||} Maki Kawai,[§] Yousoo Kim,[‡] and Young Kuk^{*,†}


[†]Department of Physics and Astronomy, Seoul National University, Seoul 151-747, Korea

[‡]RIKEN Advanced Science Institute, Wako, Saitama 351-0198 Japan

[§]Department of Advanced Materials Science, The University of Tokyo, Kashiwa, Chiba 277-8561 Japan

^{||}Department of Chemistry and Department of Electronic Chemistry, Tokyo Institute of Technology, Yokohama, Kanagawa 226-8502, Japan

[⊥]Institute of Materials Chemistry and Engineering, Kyushu University, Fukuoka 812-858, Japan

 Supporting Information

ABSTRACT: We synthesized an azobenzene derivative to demonstrate a one-dimensional molecular zipper. The formation and underlying mechanism of the molecular zipper formed by combined hydrogen-bonding and van der Waals interactions between adjacent molecules were investigated on a Au(111) surface using scanning tunneling microscopy and density functional theory calculations.

Nanometer-scale molecular structures fabricated on solid surfaces have attracted much interest in the effort to produce desired nanostructural patterns for various applications including biosensors, molecular electronics, and optoelectronic devices.^{1–4} The conformation of a molecular structure on a surface is driven by a subtle balance between molecule–surface and intermolecular interactions, typically hydrogen-bonding and/or van der Waals (vdW) interactions.^{5,6} A molecular zipper (MZ) is one of the interesting molecular structures designed to resemble natural DNA, a polymeric zipper. An MZ can be defined as a molecular structure in which molecules interlock in two directions, along the length of the zip and across it, like a human-made zipper.⁷ To date, MZs have been investigated mainly in solutions or as two-dimensionally grown forms on surfaces.^{8–11} In an effort to develop a one-dimensional (1D) MZ on a surface and study its underlying mechanism, we designed an azobenzene derivative. Here we report isolated 1D MZs formed by a combination of hydrogen-bonding and vdW interactions between adjacent azobenzene derivatives.

The experiment was performed on a Au(111) sample that had been cleaned by repeated cycles of Ar ion sputtering and annealing under ultrahigh vacuum (UHV) at a base pressure lower than 5.0×10^{-11} Torr. We synthesized an azobenzene derivative with a hexyloxy substituent at the 4 position and an ethoxy group at the 4' position (EtO–Az–OHx) (Figure 1; also see the Supporting Information). EtO–Az–OHx molecules were deposited on a clean Au(111) surface by thermal evaporation at 380 K under UHV conditions. The Au(111) substrate was maintained at room temperature during deposition. Measurements were performed using a home-built scanning tunneling microscope (STM) at various temperatures between 20 K and room temperature. All of the STM images were acquired at 90 K.

In order to understand the electronic and geometrical details of observed the MZs, we performed first-principles calculations based on density functional theory (DFT) with 1D periodic boundary conditions (PBCs) (see the Supporting Information, Figure S1). Net atomic charges were evaluated using the density-derived electrostatic and chemical (DDEC) method.¹² Computational details are provided in the Supporting Information.

Figure 2a shows a clean Au(111) surface with reconstructed herringbone structures consisting of hexagonal close-packed (hcp) and face-centered cubic (fcc) regions and herringbone ridges and elbows.¹³ Upon deposition on the Au(111) surface, EtO–Az–OHx molecules formed MZs only in fcc regions with an average width of 2.4 ± 0.1 nm, as shown in Figure 2b. The STM images do not show bent structures or branched shapes of the MZs, which can be seen more clearly in Figure 2c, a close-up image of the MZ. Also observed were MZs crossing the herringbone ridges, as shown in Figure 2d, which reveals the fact that MZ growth was not confined to the reconstructed structure of the Au(111) surface. Since the width of the MZs is slightly larger than that of the hcp region on a reconstructed Au(111) surface, MZs nucleated mainly on the fcc regions.

MZs in the fcc regions and crossing the herringbone ridges both displayed the internal structure that is clearly visible in Figure 3a. Each EtO–Az–OHx molecule in the MZs appears as an asymmetric rod shape with a node structure corresponding to the N=N bond.^{14–17} The two protrusions on either side of the node are attributed to the phenyl rings, which are brighter than the alkyl chains. Each molecule in the MZ lies along the $\{101\}$ direction according to the threefold symmetry of the Au(111) substrate, which brought about the growth direction of the MZs.

Figure 3b shows that the center-to-center spacing of phenyl rings in adjacent molecules is 6.2 ± 0.2 Å, which is much smaller than that of phenyl rings in adjacent azobenzene molecules in the molecular chain formed on the Au(111) surface (~ 8 Å).¹⁴ This indicates that MZ formation is the result of strong intermolecular interactions brought about by derivatization of an azobenzene molecule. The assembled model in Figure 3c is proposed on the basis of STM observations showing the interdigitation of the molecules in the MZ. The two phenyl rings of the EtO–Az–OHx molecule in Figure 3c are designated P1 (EtO) and P2 (OHx).

Received: April 6, 2011

Published: May 18, 2011

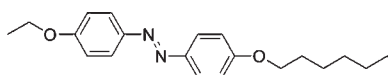


Figure 1. Chemical structure of EtO–Az–OHx.

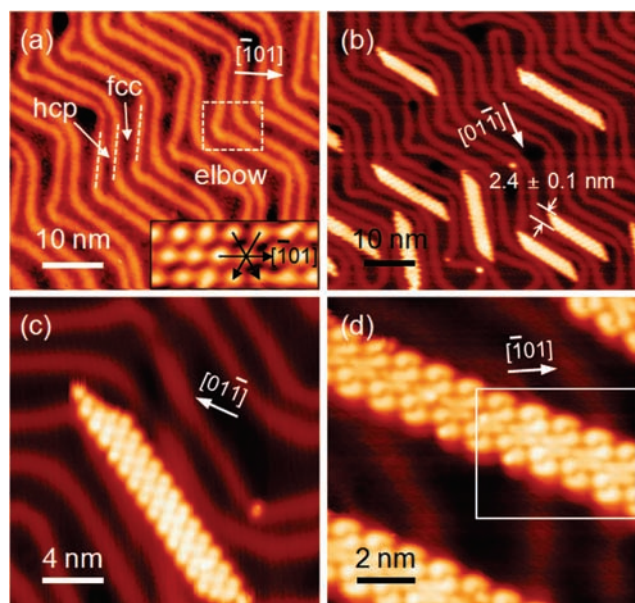


Figure 2. (a) STM image of the reconstructed Au(111) surface. There are four distinctly different types of Au atoms: hcp and fcc regions (arrows), herringbone ridges (dashed lines), and elbows (dashed box). Inset: magnified image showing the close-packed structure of Au ($V_s = 20$ mV, $I_t = 3.5$ nA). (b) STM image of MZs formed by EtO–Az–OHx molecules ($V_s = -1.0$ V, $I_t = 40$ pA). (c) Close-up STM image of an MZ confined to an fcc region of the Au(111) herringbone reconstruction ($V_s = -1.0$ V, $I_t = 0.1$ nA). (d) Close-up STM image of MZs crossing the herringbone ridges ($V_s = -1.0$ V, $I_t = 0.1$ nA).

The figure shows that two kinds of intermolecular interactions act in the formation of the MZs: vdW interactions between two alkyl chains connected to P2 rings and two C–H···O hydrogen-bonding interactions between P1 of one molecule and P2 of an adjacent molecule, as indicated by the dashed lines.

In order to understand the driving force for the EtO–Az–OHx MZ structure, we examined several MZ structures and compared their stabilities using DFT calculations. Considering two intermolecular interactions (vdW and hydrogen-bonding interactions) and the symmetry of the molecular structure, only two kinds of molecular MZs are possible (designated “A” and “B” in Figure 4). “A” has the structure that we observed in the STM images. Figure 4a,b also show the calculated electron charge densities of “A” and “B”. The electron density map clearly indicates that the ether oxygen atoms have the highest electron density, providing the hydrogen-bonding interactions between two neighboring molecules. This is also supported by the atomic charges of the EtO–Az–OHx molecule, where the interacting oxygen and hydrogen atoms carry negative (approximately $-0.3e$) and positive (approximately $+0.1e$) charges, respectively (see the Supporting Information, Figure S2). The change in atomic charge during MZ formation is a mere $0.02e$. While “A” is composed of only one type of C–H···O hydrogen bonds, namely, P1–P2, “B” has two types of hydrogen bonds, P1–P1 and P2–P2, alternately located in

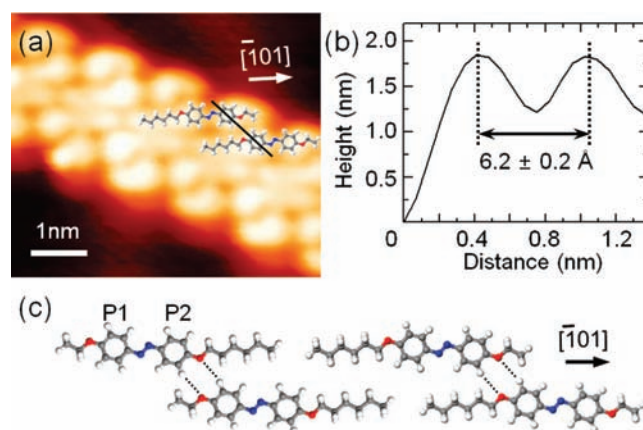


Figure 3. (a) Close-up STM image of the region enclosed by the white box in Figure 2d ($V_s = -1.0$ V, $I_t = 0.1$ nA). (b) Cross section of the two adjacent EtO–Az–OHx molecules along the black line in (a). (c) Proposed MZ structure. The dashed lines indicate C–H···O hydrogen bonds.

each molecular row. Consequently, the alkyl chains in one molecular row of “A” are aligned in the same direction and face each other with the alkyl chains of the neighboring row in an interdigitating pattern. However, those of “B” are alternately positioned within and outside of MZs. Figure 4 uses red and yellow arrows to show the hydrogen-bonding and vdW interactions, respectively. With this we surmise that formation of “A” is preferable to “B” because half of the alkyl chains in “B” are unable to take advantage of vdW interactions. The calculated results confirmed that “A” has a higher binding energy by 12 meV per molecule, although DFT calculations do not take full account of dispersion forces between molecules. In addition, the calculated width of “A” is 2.3 nm, which agrees well with the experimentally observed value (Figure 2b). The hydrogen bond distances of “A” (2.74–2.75 Å) are shorter than those of “B” (2.74–2.88 Å) (see the Supporting Information, Figure S3), which means that the hydrogen-bonding interactions in “A” are stronger than those in “B”. This relative stability of “A” results from the synergetic effect of the hydrogen-bonding and vdW interactions. Therefore, we conclude that the formation of 1D MZs can be achieved through well-balanced intermolecular interactions (i.e., hydrogen-bonding and vdW interactions) during molecular deposition on the Au(111) surface.

We next considered the effects of the EtO–Az–OHx structure and the substrate on the formation of 1D MZs. We first noted that attaching alkyl chains with two different chain lengths to the azobenzene led to the formation of 1D MZs. If the lengths of the two alkyl chains are the same, two-dimensional growth with vdW interactions might be preferable. We also expect that if we were to change the length of the alkyl chain connected to P2, we might be able to control the width of the 1D MZ. Second, we examined the influence of the substrate on MZ growth. It has often been observed that the phenyl rings of azobenzene molecules are positioned on hollow sites of Au or Cu atoms.^{16–18} However, the center-to-center spacing of two phenyl rings as shown in Figure 3b does not fit the surface lattice parameters well, which suggests that the MZ structure is not commensurate with the substrate and that intermolecular interactions might play a more decisive role in the fabrication of the molecular architectures. When an EtO–Az–OHx molecule reaches the surface, it interacts with the substrate, occupying a usual

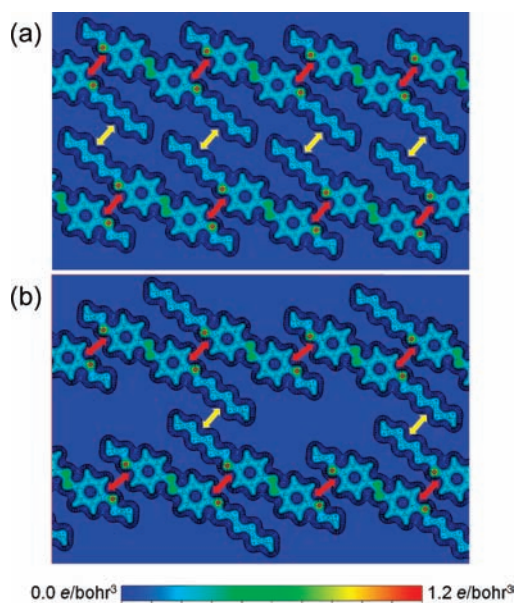


Figure 4. Electron densities of (a) “A” and (b) “B”. The red and yellow arrows indicate hydrogen-bonding and vdW interactions, respectively. The contours are drawn at logarithmic intervals of $1.0 \times 10^{1/5} e/\text{bohr}^3$.

adsorption site, such as a phenyl ring on a hollow site. However, when the next molecule is added, the intermolecular interactions become dominant, and with every additional molecule added, the molecule strays a little farther from the original adsorption site. Thus, individual molecules in the MZ may not be fully aligned with the substrate, even though the MZ is properly aligned with the high-symmetry directions of the substrate. Therefore, it is our observation in this work that the MZ can be fabricated on various solid substrates that have only weak interactions with adsorbates.¹⁹

In summary, we have presented the formation of MZs of azobenzene derivatives as studied by STM observation and DFT calculations. Formation of the MZs is driven by the intermolecular interactions consisting of vdW interactions between two alkyl chains and C–H···O hydrogen-bonding interactions, and the molecule–substrate interactions affect the direction of the MZ on the substrate. The results of the present study may provide a novel way of controlling the width of the MZ by tuning the lengths of the alkyl chains.

■ ASSOCIATED CONTENT

S Supporting Information. Details of the synthesis of the EtO–Az–OHx molecule, computational details, selected atomic charges, selected geometrical parameters, and Cartesian coordinates of optimized MZs. This material is available free of charge via the Internet at <http://pubs.acs.org>.

■ AUTHOR INFORMATION

Corresponding Author
ykuk@phy.snu.ac.kr

Present Addresses

[#]The Institute for Solid State Physics, The University of Tokyo, Kashiwa-no-ha, Kashiwa 277–8581, Japan.

■ ACKNOWLEDGMENT

This work was financially supported in part by a Grant-in-Aid for Scientific Research on Priority Areas “Electron Transport through a Linked Molecule in Nanoscale” and a Grant-in-Aid for Scientific Research (S) “Single Molecule Spectroscopy Using Probe Microscope” from the Ministry of Education, Culture, Sports, Science, and Technology (MEXT), Japan, and in part by the Global COE Program “Chemistry Innovation through Cooperation of Science and Engineering”, MEXT, Japan. We acknowledge support by the National Research Foundation of Korea (NRF-2006-0093847 and NRF-2010-00349). We are grateful for the computational resources of the RIKEN Integrated Cluster of Clusters (RICC) supercomputer system. J.J. kindly acknowledges the International Program Associate (IPA) of RIKEN for financial support. We also wish to thank David W. Chapmon for carefully reading the manuscript.

■ REFERENCES

- (1) Joachim, C.; Gimzewski, J. K.; Aviram, A. *Nature* **2000**, *408*, 541.
- (2) De Feyter, S.; De Schryver, F. C. *Chem. Soc. Rev.* **2003**, *32*, 139.
- (3) Barth, J. V.; Costantini, G.; Kern, K. *Nature* **2005**, *437*, 671.
- (4) Otero, R.; Rosei, F.; Besenbacher, F. *Annu. Rev. Phys. Chem.* **2006**, *57*, 497.
- (5) Barth, J. V.; Weckesser, J.; Cai, C.; Günter, P.; Bürgi, L.; Jeandupeux, O.; Kern, K. *Angew. Chem., Int. Ed.* **2000**, *39*, 1230.
- (6) Böhringer, M.; Schneider, W.-D.; Berndt, R. *Angew. Chem., Int. Ed.* **2000**, *39*, 792.
- (7) Munro, O. Q.; du Toit, K.; Drewes, S. E.; Crouch, N. R.; Mulholland, D. A. *New J. Chem.* **2006**, *30*, 197.
- (8) Bisson, A. P.; Carver, F. J.; Eggleston, D. S.; Haltiwanger, R. C.; Hunter, C. A.; Livingstone, D. L.; McCabe, J. F.; Rotger, C.; Rowan, A. E. *J. Am. Chem. Soc.* **2000**, *122*, 8856.
- (9) Tao, F.; Bernasek, S. L. *J. Am. Chem. Soc.* **2005**, *127*, 12750.
- (10) Vonau, F.; Suhr, D.; Aubel, D.; Bouteiller, L.; Reiter, G.; Simon, L. *Phys. Rev. Lett.* **2005**, *94*, No. 066103.
- (11) Shu, L.; Mu, Z.; Fuchs, H.; Chi, L.; Mayor, M. *Chem. Commun.* **2006**, 1862.
- (12) Manz, T. A.; Sholl, D. S. *J. Chem. Theory Comput.* **2010**, *6*, 2455.
- (13) Barth, J. V.; Brune, H.; Ertl, G.; Behm, R. *J. Phys. Rev. B* **1990**, *42*, 9307.
- (14) Kirakosian, A.; Comstock, M. J.; Cho, J.; Crommie, M. F. *Phys. Rev. B* **2005**, *71*, No. 113409.
- (15) Henzl, J.; Mehlhorn, M.; Gawronski, H.; Rieder, K.-H.; Morgenstern, K. *Angew. Chem., Int. Ed.* **2006**, *45*, 603.
- (16) Choi, B.-Y.; Kahng, S.-J.; Kim, S.; Kim, H.; Kim, H. W.; Song, Y. J.; Ihm, J.; Kuk, Y. *Phys. Rev. Lett.* **2006**, *96*, No. 156106.
- (17) Miwa, J. A.; Weigelt, S.; Gersen, H.; Besenbacher, F.; Rosei, F.; Linderoth, T. R. *J. Am. Chem. Soc.* **2006**, *128*, 3164.
- (18) Kim, H. W.; Han, M.; Shin, H.-J.; Lim, S.; Oh, Y.; Tamada, K.; Hara, M.; Kim, Y.; Kawai, M.; Kuk, Y. *Phys. Rev. Lett.* **2011**, *106*, No. 146101.
- (19) Vonau, F.; Aubel, D.; Bouteiller, L.; Reiter, G.; Simon, L. *Phys. Rev. Lett.* **2007**, *99*, No. 086103.